JOURNAL OF CATALYSIS 130, 588–596 (1991)

Solving Dynamic Equations for the Size Distribution of Supported Metal Catalysts

RAYMOND C. EVERSON,* DAVID EYRE,†,[1] AND COLIN J. WRIGHT‡

*Department of Chemical Engineering, Potchefstroom University for CHE, Potchefstroom, Republic of South Africa; †Department of Mathematics and Applied Mathematics, Potchefstroom University for CHE, Vanderbijpark, Republic of South Africa; and ‡Department of Computational and Applied Mathematics, University of the Witwatersrand, WITS 2050, Republic of South Africa

Received August 30, 1990; revised February 21, 1991

A simple kinetic model for the growth of catalytic metal crystallites on a support is investigated. Results for an exactly solvable coalescence model with initial condition consistent with experiment shows that the similarity solution does not provide an accurate description of the particle size distribution. A numerical solution of the kinetic equation is shown to be in excellent agreement with experimental data. The model can be used to provide useful information concerning the underlying mechanism responsible for sintering. © 1991 Academic Press, Inc.

INTRODUCTION

A complete understanding of crystallite growth during the sintering process, occurring when supported metal crystallites are exposed to high temperatures, is limited by our ability to obtain accurate solutions of equations that describe the process as well as the prediction of particle (crystallite) size distributions (PSD) that agree with experimental data. Previous studies (*1–4*) based upon measurement and prediction of surface area as a function of treatment time, in the form of a power law relationship, is unsatisfactory in order to differentiate between models of sintering by coalescence and/or atomic migration (*5, 6*). A recent paper by Wu and Phillips (*6*) reported modelling results based upon a model proposed by Ruckenstein and Dadyburjor (*7*), but was unable to predict experimental PSDs because of the limitation of the numerical method used. Campbell *et al.* (*5*) carried out Monte Carlo simulations of sintering and redispersion and also presented qualitative results in agreement with experimental observations.

In the present study a coalescence model of sintering is investigated. It is shown that a model based on an accurate solution (*8*) of a partial integro-differential equation can accurately describe the growth of catalytic particles distributed on a support. The strength of the present method rests in the fact that it can treat a wide class of initial distributions including distributions that are given only as experimental data. A description of a simple test example is given together with an application of the sintering process involving palladium on alumina.

COALESCENCE MODEL FOR CRYSTALLITE GROWTH

It is assumed that particles of metal migrate across the surface, due to thermal motion, and grow by collision and coalescence. In order to construct a mathematical model of this process it is necessary to make a number of assumptions concerning the system: (i) There is a homogeneous distribution of particles and a sufficiently low surface density that only collision between pairs leads to coalescence, (ii) the nature of the surface is such that all particles are free to migrate, (iii) atomic sizes are small com-

[1] To whom correspondence should be addressed.

0021-9517/91 $3.00

pared with metal particle sizes. Assumption (iii) is made so that the computational difficulties associated with the inclusion in the model of particles comprising a large number of atoms can be overcome.

Under these assumptions the evolution of the PSD is governed by the partial integro-differential equation

$$\frac{\partial}{\partial t}N(v, t) = \int_0^{v/2} N(V, t)N(v - V, t)K(V, v - V)\,dV - N(v, t)\int_0^{\infty} N(V, t)K(V, v)\,dV. \quad (1)$$

Here $N(v, t)\,dv$ is the average number of crystallites with volume between v and $v + dv$ on unit surface area of support at time t. The kernel $K(V, v)$ describes the geometry and dynamics of the collection mechanism for two particles of volume V and v and is a symmetric function of its two arguments.

Equation (1) is a balance equation where the first term on the right-hand side represents the increase in the number of particles of volume v by coalescence of two smaller particles, and the second term represents the loss of particles of volume v by coalescence with a particle of any other volume. This basic equation can be modified to include other mechanisms such as condensation and evaporation of particles (*9*). It is known that the deterministic equation (1) approximately describes a stochastic process (*10*).

The total average number, $M_0(t)$, and volume, M_1, of particles on unit area of support is given by the moments

$$M_0(t) = \int_0^{\infty} N(v, t)\,dv, \quad (2)$$

and

$$M_1 = \int_0^{\infty} vN(v, t)\,dv. \quad (3)$$

The fact that M_1 is a constant is seen by integrating Eq. (1). Thus Eq. (1) guarantees that the total volume of metal on the surface is conserved. The initial number of particles is denoted by $N_0 = M_0(0)$.

For simplicity the particles are assumed to be hemispherical. For hemispherical particles a simple relationship exists between the volume v and the radius r of each particle so that v can be replaced by r as an independent variable. The kernel $K(r, R)$ is taken to be the form given by Ruckenstein and Pulvermacher (*3*). Here it is assumed that the diffusion coefficient $D(r, R)$ has a simple dependence on the two particle radii r and R so that

$$K(r, R) = c_k(r^k + R^k). \quad (4)$$

The value of exponent k corresponds to two limiting cases: For $k \leq 0$ the interaction between the metal particles and the support is strong so that diffusion is the rate-determining process (this is referred to as the diffusion-controlled case). On the other hand for $k > 0$ the interaction is weak and the diffusion time is short compared with coalescence (this is referred to as the sintering-controlled case). For the diffusion-controlled case the kernel depends on a small scale time θ associated with the diffusion of particles across the surface. This dependence on time is weak provided that (*3*)

$$\ln(4T) \gg 1, \quad (5)$$

where the dimensionless time $T = 4\pi D\theta/\rho$ and $\rho = r + R$ is the collision distance.

The total exposed surface area of metal on unit area of support is given by

$$S(t) = \sigma\int_0^{\infty} v^{2/3}N(v, t)\,dv, \quad (6)$$

where for hemispherical particles the shape constant is $\sigma = (18\pi)^{1/3}$. Given the kernel in Eq. (4) Ruckenstein and Pulvermacher (*3*) have shown that the exposed surface area of metal approximately satisfies a simple equation of the form

$$\frac{dS}{dt} = -\alpha_k S^{4-k}. \quad (7)$$

Thus measurement of the exposed surface area of metal as a function of time could yield information on the mechanism respon-

sible for sintering. This behaviour is not very satisfactory as mentioned above.

NUMERICAL METHOD OF SOLUTION

Equation (1) can be written in a dimensionless form. Because particle volumes may vary over many orders of magnitude it is necessary to develop an approach that can treat particles of widely differing sizes. For this purpose the volume v is transformed to a dimensionless variable q on the finite interval $[-1, 1]$,

$$v = \zeta\left(\frac{1+q}{1-q}\right). \tag{8}$$

Here ζ is a volume parameter which can be chosen so that the solution of Eq. (1) is distributed in a reasonable way over the interval $[-1, 1]$. The value of ζ remains fixed throughout the calculation. On introducing a diffusion parameter χ that defines a natural scale for the kernel, the dimensionless kernel becomes

$$\beta(Q, q) = \frac{1}{\chi} K(V, v). \tag{9}$$

(In particular for a kernel of the form (4) one can take $\chi = c_k$.). Introducing a dimensionless time

$$\tau = \chi N_0 t, \tag{10}$$

and dimensionless dependent variable

$$\nu(q, t) = \frac{\zeta}{N_0} N(v, t), \tag{11}$$

Eq. (1) becomes

$$\frac{\partial}{\partial \tau}\nu(q, \tau) = \int_{-1}^{q(v/2)} \nu(Q, \tau)\nu(u, \tau)\beta(Q, u)\omega(Q)\, dQ - \nu(q, \tau) \int_{-1}^{1} \nu(Q, \tau)\beta(Q, q)\omega(Q)\, dQ, \tag{12}$$

where

$$u \equiv u(q, Q) = \frac{2(q - Q) - (1 - q)(1 - Q)}{2(q - Q) + (1 - q)(1 - Q)}, \tag{13}$$

is the transformed volume difference, $v - V$, and

$$\omega(q) = \frac{2}{(1 - q)^2}. \tag{14}$$

The approach taken in the present paper is to solve Eq. (12) using a technique based on a collocation method and a finite element basis (*8*). A brief description of the numerical method is now given.

Introducing a cut off parameter q_c the interval $[-1, q_c]$ is partitioned using n interior nodes; two nodes are fixed at -1 and q_c, respectively. On this partition one defines $(n + 2)$ cubic B-splines (*11*), B_i, and writes

$$\nu(q, \tau) \approx \sum_{i=0}^{n+1} f_i(\tau) B_i(q), \tag{15}$$

Coefficients $f_i(\tau)$ are sought that approximate the solution of Eq. (12). These coefficients satisfy the equation

$$\frac{\partial}{\partial \tau}\sum_{i=0}^{n+1} f_i(\tau)B_i(q) = \sum_{i=0}^{n+1}\sum_{j=0}^{n+1} f_i(\tau)f_j(\tau)c_{ij}(q), \tag{16}$$

where coefficients $c_{ij}(q)$ are given by moment integrals

$$c_{ij}(q) = \int_{-1}^{q(v/2)} B_i(u)B_j(Q)\beta(Q, u)\omega(Q)\, dQ - B_i(q)\int_{-1}^{1} B_j(Q)\beta(Q, u)\omega(Q)\, dQ. \tag{17}$$

Equation (16) is reduced to a system of ordinary differential equations by collocating at $(n + 2)$ points. These points are chosen to coincide with the nodes of the cubic spline, plus two additional points which are placed midway between the nodes defining each end interval. A fully implicit one-step method is used to solve the system of ordinary differential equations.

AN EXACTLY SOLVABLE MODEL

Some insight into the model can be gained from an exact analytic solution of Eq. (1). Unfortunately such solutions can be found only for special choices of the kernel and

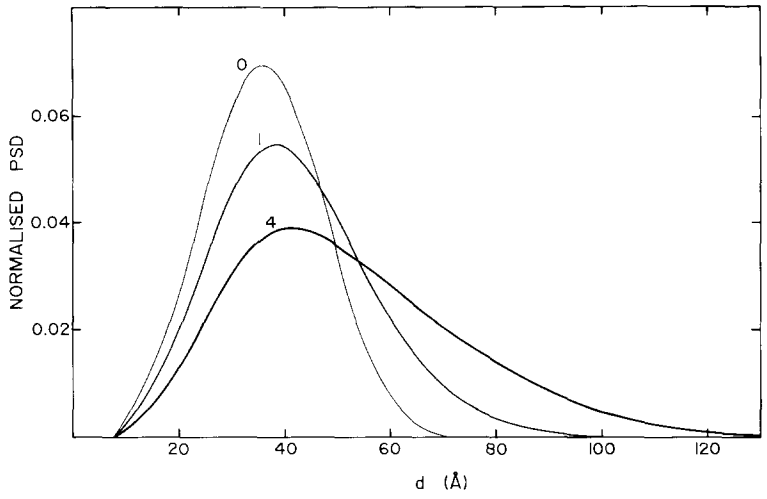

FIG. 1. Normalised PSD for the test problem. Curves are labeled by the time in hours. The difference between exact and computed solutions is too small to show up in the figure.

initial condition (*12*). Such an initial condition that is consistent with experiment has the form

$$N(v, 0) = \frac{4N_0 v}{v_0} \exp\left(-\frac{2v}{v_0}\right), \tag{18}$$

where N_0 and v_0 are free parameters denoting the initial number and initial average volume of particles, respectively.

For a constant kernel $K(v, V) = \gamma$ Eq. (1) has the solution (*12*) (the notation $M_0 \equiv M_0(t)$ is used in what follows)

$$N(v, t) = 2\frac{M_0^2}{M_1}\frac{1}{\sqrt{1 - M_0/N_0}} e^{-2v/v_0} \sinh\left(\sqrt{1 - M_0/N_0}\,\frac{2v}{v_0}\right), \tag{19}$$

with moments

$$M_0 = \frac{2}{2 + \gamma N_0 t}, \tag{20}$$

and

$$M_1 = N_0 v_0. \tag{21}$$

Substituting Eq. (19) into Eq. (6) gives

$$S(t) = \frac{1}{3}\frac{\Gamma(\frac{2}{3})}{2^{2/3}} \sigma M_1^{2/3} M_0^{1/3} \left[\frac{(1 + R)^{5/3} - (1 - R)^{5/3}}{R}\right], \tag{22}$$

$R = \sqrt{1 - M_0/N_0}$, and for $S_0 \equiv S(0)$,

$$S_0 = \frac{1}{3}\frac{\Gamma(2/3)}{2^{2/3}} \sigma N_0 v_0^{2/3}. \tag{23}$$

A number of important results concerning the solution of Eq. (1) have been obtained by means of a similarity solution. The idea behind this approach is to assume something about the solution function $N(v, t)$ and in this way obtain an equation for the assumed form that is easier to solve than Eq. (1). The transformation is

$$\psi(\eta) = \frac{A^2}{B}\frac{M_1}{M_0^2} N(v, t), \tag{24}$$

$$\eta = \frac{B}{A}\frac{M_0}{M_1} v, \tag{25}$$

where it follows from the definition of the moments (Eqs. (2) and (3)) that

$$A = \int_0^\infty \psi(\eta)\, d\eta, \tag{26}$$

and

$$B = \int_0^\infty \eta\psi(\eta)\, d\eta. \tag{27}$$

In the case of a constant kernel, the transformation (24) and (25) leads to an ordinary differential equation of the form

$$\eta \frac{d}{d\eta}\psi(\eta)\left(\int_0^\infty \psi(\tilde{\eta})\,d\tilde{\eta}\right) + \int_0^\eta \psi(\tilde{\eta})\psi(\eta - \tilde{\eta})\,d\tilde{\eta} = 0. \quad (28)$$

For the boundary condition $\psi(0) = 1$, Eq. (28) has the solution

$$\psi(\eta) = e^{-\eta}. \quad (29)$$

It remains to be shown that the similarity solution (29) satisfies Eq. (1). For initial distribution (18) and constant kernel, the exact solution (19) of Eq. (1) leads to the function

$$\psi(\eta) = 2\left(1 + \frac{2}{\tau}\right)^{1/2} e^{-(2+\tau)\eta} \sinh\left[\left(\frac{2}{2+\tau}\right)^{1/2}(2+\tau)\eta\right], \quad (30)$$

where the dimensionless time $\tau = \gamma N_0 t$. For large τ and

$$\eta \gg \frac{1}{2(1+\tau)}, \quad (31)$$

the similarity solution (29) is obtained. Note, however, that if η is sufficiently small and the inequality of Eq. (31) is not satisfied then Eq. (29) is not a solution of Eq. (1). Indeed Eq. (30) satisfies the boundary condition $\psi(0) = 0$.

TABLE 1

Exact (E) and Calculated (C) Moments for the Test Problem

t (h)	$M_0 = 10^{18}$		$M_1 \times 10^{22}$ (Å^3)		S (m^2)	
	E	C	E	C	E	C
0	3.70	—	8.77	—	111.1	111.1
1	1.75	1.79	8.77	8.77	84.7	85.1
2	1.15	1.17	8.77	8.77	73.0	73.3
3	0.85	0.87	8.77	8.75	65.9	66.0
4	0.68	0.69	8.77	8.67	60.9	60.7

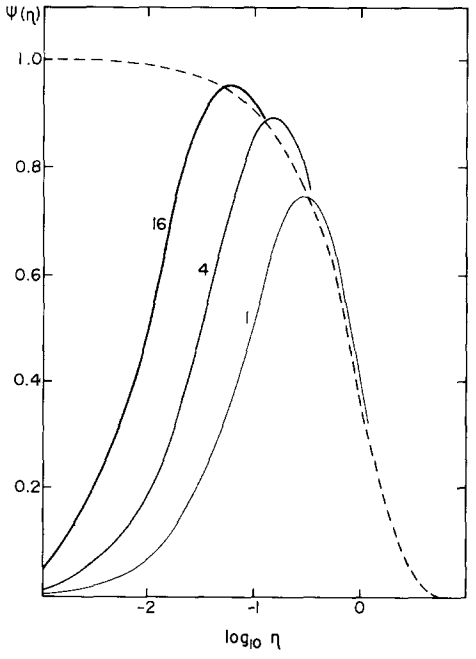

FIG. 2. Dimensionless variable $\psi(\eta)$. Broken curve is the function $e^{-\eta}$. Solid curves are obtained for the test problem and are labelled by the time in hours.

RESULTS AND DISCUSSION

The initial distribution chosen for the present calculations is that used by Chen and Ruckenstein (*13*) in their study of sintering of palladium on an alumina model catalyst. It should be remarked that the experimental PSD is given in the form of a histogram where the percentage of particles having diameters in a particle size of width 5 Å is presented. In order to compute results using Eq. (1) it is necessary to first fit this data to a smooth curve using cubic spline approximation with knots positioned at the center of each interval. It is assumed that 1 g of metal is distributed over the support surface.The surface area of support is denoted by L^2. In the diffusion-controlled case L^2 is restricted by the condition in Eq. (5), otherwise it is a "free" parameter. A spline fit to the initial distribution at 650°C yields moments $N_0 = 3.70 \times 10^{18}$ and $M_1 = 8.77 \times 10^{22}$ Å^3 of metal on L^2 surface area of support.

TABLE 2

Calculated Ratios S/S_0 for Different Kernels $K(r, R) = c_k(r^k + R^k)$

t	$c_2 = 3 \times 10^{-22}$	$c_1 = 9 \times 10^{-21}$	$c_0 = 6 \times 10^{-19}$	$c_{-1} = 10^{-17}$	$c_{-2} = 3 \times 10^{-16}$	Exp (*13*)
0.5	0.903	0.889	0.859	0.822	0.797	0.90
1	0.823	0.808	0.772	0.737	0.718	0.67
4	0.539	0.565	0.554	0.551	0.561	0.56
8	0.365	0.483	0.455	0.469	0.492	0.55
20	0.170	0.286	0.321	0.372	0.410	0.51

Note. The best fit to the PSD is obtained with $k = -1$.

The test problem is considered first. This problem serves as a benchmark calculation. The special form of the initial condition (18) means that this function is completely specified by just two parameters N_0 and M_1. The remaining parameter γ is chosen to approximately describe the experimental data (*13*) and is taken to be $\gamma = 6 \times 10^{-19} L^2 \text{ h}^{-1}$.

Figure 1 shows the change in the PSD as a function of the particle diameter where each curve is normalized so that the area under the curve is unity. The difference between the exact and computed solutions is too small to show up in the figure. Table 1 shows the comparison between exact (E) and computed (C) moments as well as the exposed surface area of metal assuming hemispherical particles.

Figure 2 shows the dimensionless variable $\psi(\eta)$. The broken curve is the function $\psi(\eta) = e^{-\eta}$ which is an exact solution for all times of the Eq. (1) when the initial condition is a simple exponential. The solid curves illustrate the time dependence of $\psi(\eta)$ when the initial condition is given by Eq. (18). Here each curve is labeled by the time in hours. As time increases the agreement with the broken curve moves to smaller values of η in agreement with the inequality of Eq. (31). The fact that these curves alter their shape over a typical time scale for sintering is evidence that the simi-

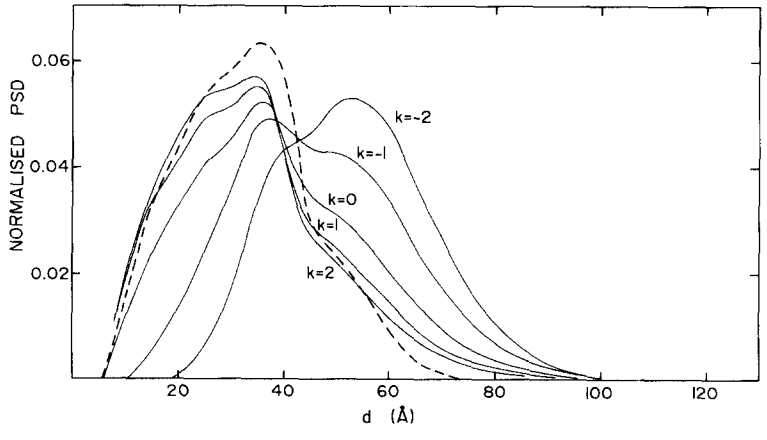

FIG. 3. Normalised PSD for an initial condition fitted to experiment (*13*). Broken curve is the normalised initial function. Solid curves are the PSD after 1 h using the kernel in Eq. (4). Each curve is labeled by the exponent k. The constant c_k is given in Table 2.

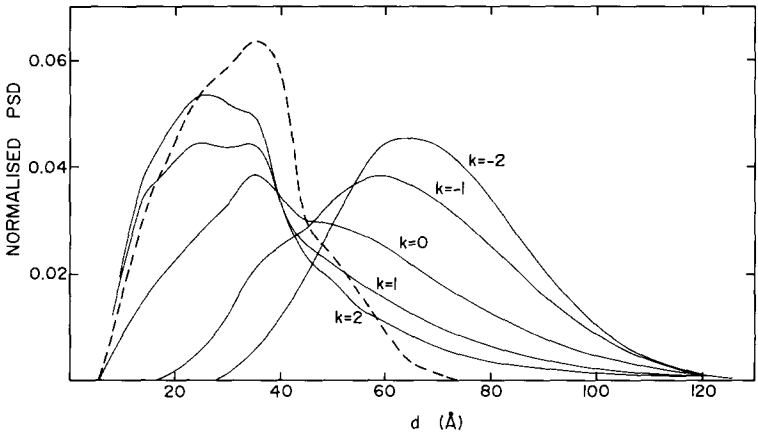

FIG. 4. Same as in Fig. 3 but with solid curves showing the PSD after 4 h.

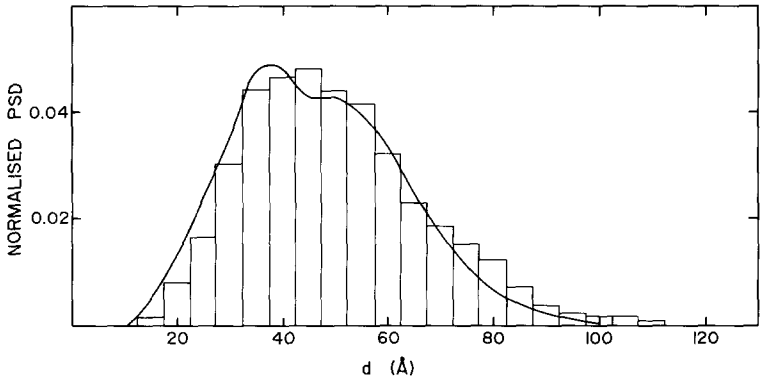

FIG. 5. Comparison of the curve labeled by $k = -1$ with the normalised experimental PSD after 1 h.

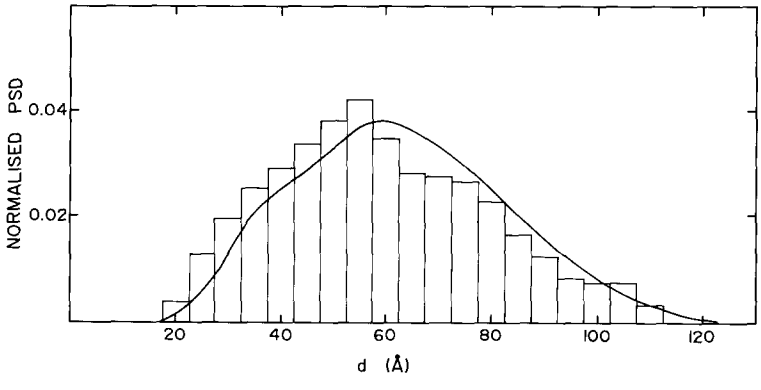

FIG. 6. Same as in Fig. 5 but after 4 h.

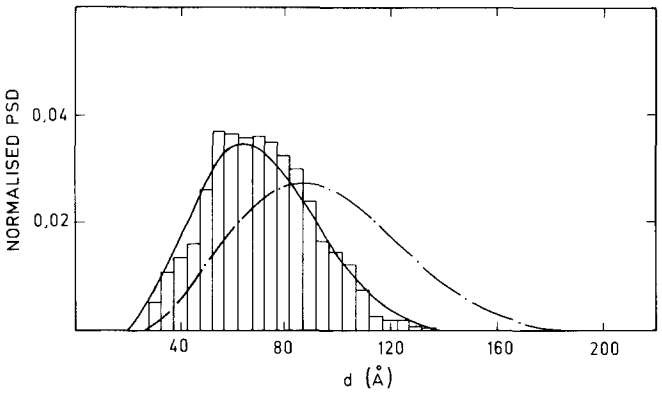

FIG. 7. Comparison of curves obtained using $c_{-1} = 10^{-17}$ (dotted) and $c_{-1} = 3 \times 10^{-18}$ (solid) with the normalised experimental PSD after 20 h.

larity solution cannot be trusted to give reliable information on the PSD. This would appear to be especially true for particles at the small particle end of the spectrum.

In order to investigate the PSD in detail, use is made of the experimental data on the initial distribution. For this initial function there is no analytic solution of Eq. (1) so one must rely on the accuracy of the numerical procedures. Table 2 shows the ratio of exposed surface areas, $S(t)/S_0$, computed using the kernel form in Eq. (4) with the exponent k ranging from 2 to -2 and c_k chosen so that the decrease in the exposed surface area after 4 h agrees approximately with experiment (*13*). It should be remarked that this quantity is independent of the shape parameter σ. As can be seen from the table, one can deduce very little about the mechanism responsible for sintering. The situation is different for the PSD. Figures 3 and 4 show the PSD after 1 and 4 h, respectively. Each curve is labelled by the exponent k used in the kernel. These curves are greatly different from one another even though they yield approximately the same exposed surface area of metal. Indeed it is found that the curve corresponding to $k = -1$, which corresponds to a diffusion-controlled case, gives the best agreement with the experimental data. A comparison of these results with the normalised data is shown in Figs. 5 and 6.

Figure 7 shows the PSD after 20 h. Both curves correspond to $k = -1$ but have been computed using different values for the constant c_{-1}. The choice $c_{-1} = 10^{-17}$ produces a curve in disagreement with the normalized data. The ratio $S/S_0 = 0.372$ also disagrees with the experimental ratio $S/S_0 = 0.51$. By choosing the constant $c_{-1} = 3 \times 10^{-18}$ a more reasonable value of the ratio $S/S_0 = 0.501$ is obtained. The resulting PSD is also in good agreement with the normalised data. The above result suggests that it would be better to assume $c_{-1} \equiv c_{-1}(t)$. Since this coefficient changes over a period of 20 h it is a slowly varying function of time.

CONCLUSIONS

Results for the PSD of a simple coalescence model have shown good agreement when compared with experimental data. The PSD provides a much clearer picture of the underlying mechanism responsible for sintering than could the change in surface area of exposed metal. For an initial distribution typical of most experiments it has been shown that the similarity solution may not provide an adequate description of the PSD, particularly for small particles, over a typical time period for sintering. This seri-

ously limits the ability of the similarity solution to provide detailed information regarding small particle growth. It does, however, provide useful information on gross features involving large particles, such as the exposed surface area.

In one specific application of the model to sintering of palladium on alumina it has been shown that the diffusion-controlled model describes the experimental PSD better than the sintering-controlled model. No such conclusions could be drawn simply from the data on the exposed surface area. The experimental PSD is described most accurately by an exponent $k = -1$. It should be noted, however, that other mechanisms such as Ostwald ripening (*14*) may also contribute to the sintering process.

REFERENCES

1. Chakraverty, B. K., *J. Phys. Chem. Solids* **28,** 2401 (1967).
2. Wynblatt, P., and Ahn, T. M., *in* "Materials Science Research" (G. C. Kuczynski, Ed.), Vol. 10, p. 83. Plenum, New York, 1975.
3. Ruckenstein, E., and Pulvermacher, B., *AIChE J.* **19,** 356 (1973).
4. Ruckenstein, E., and Pulvermacher, B., *J. Catal.* **29,** 224 (1973).
5. Campbell, W. G., Lynch, D. T., and Wanke, S. E., *AIChE J.* **34,** 1528 (1988).
6. Wu, N. J., and Phillips, J., *J. Catal.* **113,** 129 (1988).
7. Ruckenstein, E., and Dadyburjor, D. B., *J. Catal* **48,** 73 (1977).
8. Eyre, D., Wright, C. W., and Reuter, G., *J. Comp. Phys.* **78,** 288 (1988).
9. Ramabhadran, T. E., Peterson, T. W., and Seinfeld, J. H., *AIChE J.* **22,** 840 (1976).
10. Gillespie, D. T., *Atmos. Sci.* **29,** 1496 (1972).
11. de Boor, C., "A Practical Guide to Splines." Springer-Verlag, New York/Heidelberg/Berlin, 1978.
12. Scott, W. T., *J. Atmos. Sci.* **25,** 54 (1968).
13. Chen, J. J., and Ruckenstein, E., *J. Catal.* **69,** 254 (1981).
14. Wanke, S. E., *J. Catal.* **46,** 234 (1977).